

The physics of plasma jets used for fast atomic deposition

Citation for published version (APA):

Schram, D. C., Beulens, J. J., Buuron, A. J. M., Kroesen, G. M. W., Meeusen, G. J., Wilbers, A. T. M., Milojevic, D., & Vallinga, P. M. (1990). The physics of plasma jets used for fast atomic deposition. In *High temperature plasma jets in the processes of treatment of materials : international workshop, September 1990, Frunze, USSR* (pp. 1-11)

Document status and date:

Published: 01/01/1990

Document Version:

Publisher's PDF, also known as Version of Record (includes final page, issue and volume numbers)

Please check the document version of this publication:

- A submitted manuscript is the version of the article upon submission and before peer-review. There can be important differences between the submitted version and the official published version of record. People interested in the research are advised to contact the author for the final version of the publication, or visit the DOI to the publisher's website.
- The final author version and the galley proof are versions of the publication after peer review.
- The final published version features the final layout of the paper including the volume, issue and page numbers.

[Link to publication](#)

General rights

Copyright and moral rights for the publications made accessible in the public portal are retained by the authors and/or other copyright owners and it is a condition of accessing publications that users recognise and abide by the legal requirements associated with these rights.

- Users may download and print one copy of any publication from the public portal for the purpose of private study or research.
- You may not further distribute the material or use it for any profit-making activity or commercial gain
- You may freely distribute the URL identifying the publication in the public portal.

If the publication is distributed under the terms of Article 25fa of the Dutch Copyright Act, indicated by the "Taverne" license above, please follow below link for the End User Agreement:

www.tue.nl/taverne

Take down policy

If you believe that this document breaches copyright please contact us at:

openaccess@tue.nl

providing details and we will investigate your claim.

The physics of plasma jets

International Workshop
"High Temperature Plasma Jets in the
Processes of Treatment of Materials"
Sept. 1990, Frunze, USSR

THE PHYSICS OF PLASMA JETS USED FOR FAST ATOMIC DEPOSITION

D.C. SCHRAM, J.J. BEULENS, A.J.M. BUURON, G.M.W. KROESEN,
G.J. MEEUSEN, A.T.M. WILBERS, D. MILOJEVIC¹, P.M. VALLINGA²

*Department of Physics, Eindhoven University of Technology,
P.O. Box 513, 5600 MB Eindhoven, The Netherlands*

¹*Boris Kidric Institute, Belgrade, Yugoslavia*

²*KSEPL, Rijswijk, The Netherlands*

INTRODUCTION

In the past decennia many new materials and surface treatment methods have evolved by the application of plasma induced processes. This evolution has been stimulated by developments in the IC technology, in particular the (sub)micron technology. As examples etching (anisotropic and isotropic) and plasma enhanced vapour deposition, e.g. the formation of passivation layers, can be mentioned.

In the IC technology the primary goal is quality. The process rate, and with that the duration of the process, is of secondary importance. So an increasing number of investigations have been aimed at a good understanding of the mechanisms in the plasma and at the wall, both in beam and plasma experiments [1,2]. Even though this has led to major advances in the understanding of several processes, still many details need to be disentangled, in particular for plasma deposition.

For other applications than IC technology high rates can very well be essential for economic reasons. Still good overall quality has to be retained. This makes it essential to analyse the plasma physics processes which limit the rates in the process. Also it urges to detailed understanding of the actual deposition process at the surface, in other words, to relate the desired surface modification process to the desired fluxes in kind and magnitude. This part is still in its infancy because of the limited possibilities to observe the surface processes in the presence of the plasma, i.e. in deposition conditions.

To reach higher particle fluxes new developments have been made. Microwave plasmas have a larger electron density and radical formation. Even larger fluxes can be reached by total separation of plasma production and plasma treatment. In the later to be described expanding beam deposition the plasma production takes place at high (sub)atmospheric pressure. This plasma, with a high heavy particle temperature, is then expanded into vacuum. The combination of large densities and large flow velocities leads to very high particle fluxes. Consequently large deposition rates have been achieved for amorphous [3,4] and crystalline carbon layers [5], and amorphous silicon [6]. Another advantage of this method is the high dissociation degree and ionization degree. Thus, atomic ions can be

obtained rather than the molecular ions in other deposition methodologies.

At this point a comparison between this atomic ion deposition and the low pressure plasma spraying process should be mentioned. In plasma spraying the plasma provides heating and momentum to spray particles. In heavy loading conditions typically 20 mg/kJ can be deposited with growth speeds of 30 μ /s. In classical plasma deposition typically 1 nm/s with 0.1 mg/kJ is obtained. In the atomic plasma beam deposition the figures are 10² nm/s with 0.4 g/kJ. Clearly the atomic plasma beam deposition is intermediate in growth rate between classical plasma enhanced vapour deposition and low pressure plasma spraying. With further development a combination of deposition and spraying may be a very interesting possibility [7].

In the following the principle of the method will be summarized with the emphasis on the possibility to tune the nature of the fluxes to the desired ones. A two-dimensional model will be described which is primarily used to optimize the plasma source conditions. Model results will be compared with various measurements.

The paper will be concluded with a summary of the state of the art and of the potentials for further work.

PRINCIPLE OF ATOMIC PLASMA BEAM DEPOSITION

In this paper the principle will only be summarized. Further details are described in the Refs. [3,4].

The plasma is produced at high pressures in a subatmospheric flowing cascade arc (see Fig. 1). The principle reason for this is the high ionization degree and good figure of merit for the ratio of intrinsic energy flow and power input. The physics behind this is summarized in Fig. 2, in which cascaded arcs are compared with microwave plasmas and RF plasmas in electron density (and thus radical formation) and in required power density. It is clear that high density plasmas need relatively lower power densities per electron. This is due to the relatively lower radiation losses. The plasma is formed in a carrier gas, such as argon or nitrogen, and has a high degree of dissociation (nearly 100%) and degree of ionization (10-30%). A pressure difference between cathodic end (gas input, 50 scc/s) and anodic end (pumped by vacuum chamber) accelerates the plasma to sonic velocities at the typical heavy particle temperatures of 1 eV. Thus an influence of 210²⁰/s with a 4 mm bore arc and a power input of 6 kW is obtained. By injection of a monomer as C₂H₂ or SiH₄ in the arc, dissociation takes place and the atoms are ionized by direct electron impact and by non resonant charge transfer from the carrier gas ions, usually argon. This way of operation is referred to as the ionic mode.

Alternatively, the monomer can be injected after expansion of the plasma beam in the vacuum deposition chamber. First we will discuss the process in this expansion. At the nozzle-anode end of the arc, the flow becomes sonic. Subsequently, supersonic acceleration occurs, with cooling of the plasma. Then a shock develops, after which the beam widens as a consequence of particle diffusion. This diffusion is relatively slow at pressures around 100 pascal, as the radius of the plasma beam is large compared to the ion-neutral mean free path. So, even though thermal velocities and directed velocities are both in the sub-eV range, the plasma beam is directed, with the evident advantage that windows remain clear during deposition.

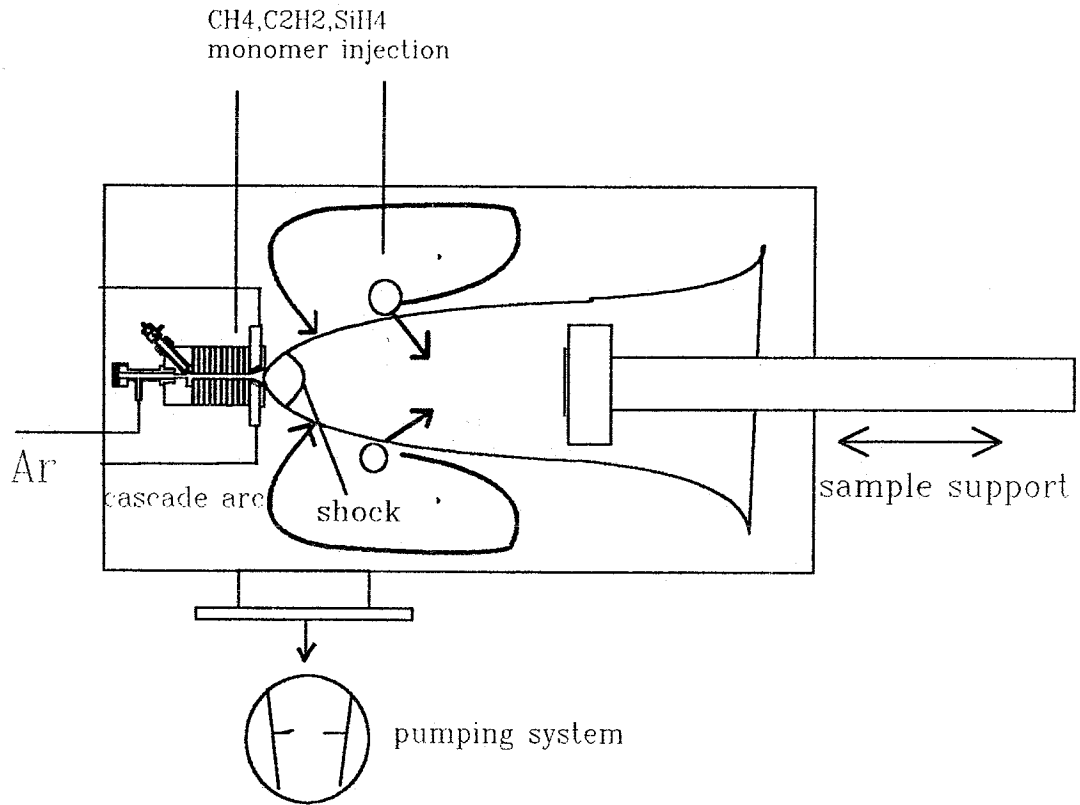


Fig. 1. Sketch of cascade arc expansion deposition apparatus.

The alternative way of injection is through a ring with many holes around the plasma. At least part of this injected gas recirculates in the outside of the chamber, after which it is sucked into the flow at the nozzle. In this way very effective mixing occurs. However, in view of the lower electron density of the expanded plasma, the dissociation will not be complete and molecular ions result from electron ionization and charge exchange with Ar⁺ ions. Therefore, in this mode there is a larger similarity with the classical RF method of plasma deposition (with larger reactivity, though). This mode will be denoted as quenched mode of operation.

An explicit disadvantage of this mode is the occurrence of dissociative recombination. This recombination process is the only effective recombination process and is 5 to 6 orders of magnitude more probable than radiative recombination. Hence, the expansion process differs vastly for atomic and molecular gases. In atomic use the plasma beam is brighter and extends much further. In order to choose between the ionic and quenched modes of operation, it is essential to know which kind of particles (ions respectively radicals) determine the deposition process. Another point of future consideration is the importance of vibrational excitation of molecular fragments, in particular for processes at the wall.

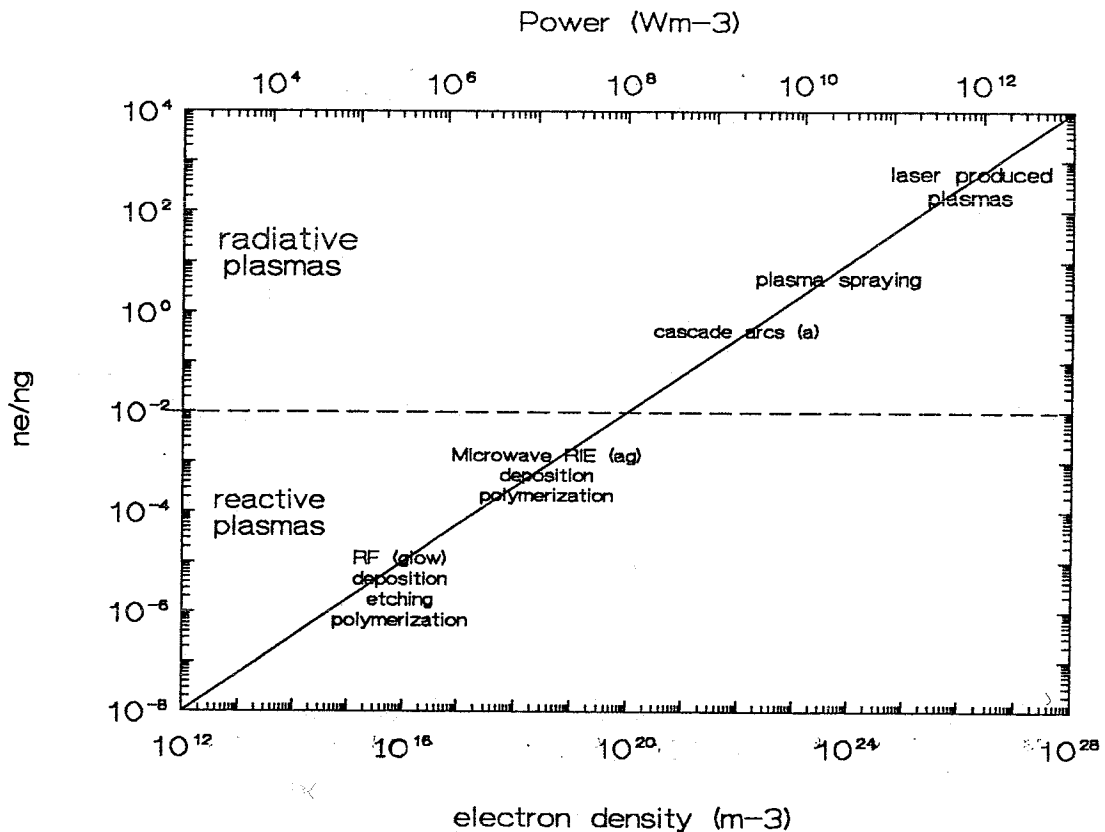


Fig. 2. Plot of various plasmas in terms of ionization degree (ratio of electron density and neutral density), electron density and power density).

CASCADE ARC PLASMA SOURCE

It is clear that the principle of the method is to produce a highly ionized strong flowing plasma with minimum power. As the material to be deposited can be charged by charge exchange further downstream, it is sufficient to optimize for an atomic ion plasma only. Up to now arcs of 4 mm cross section have been used. It is possible that a variation of the arc cross section with distance from the cathode may give better results. At the beginning of the arc the pressure is high and diffusion slow. As also a high current density is required a small cross section would be optimum. Further downstream to the anode the heating requirements are smaller and diffusion is faster, so a larger diameter may be more appropriate.

In order to address these questions a two-dimensional model has been developed [8] based on mass, momentum and energy conservation. This model will be summarized shortly and results will be compared with several measured data.

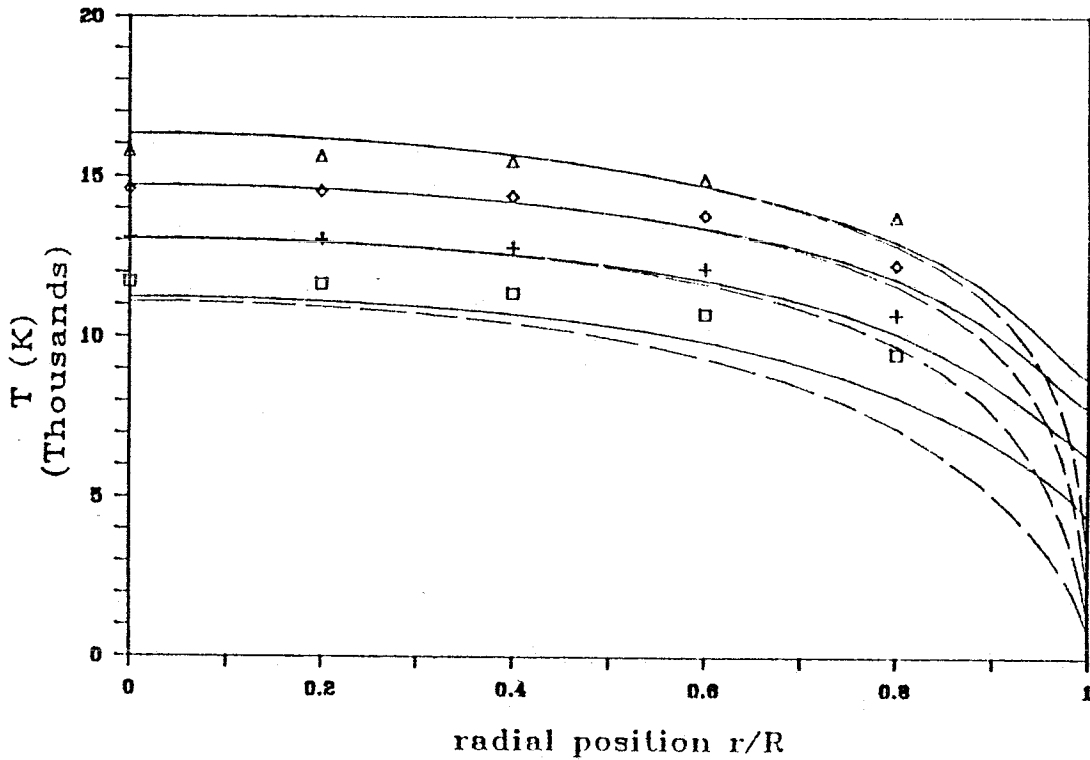


Fig. 3. Stagnation arc: electron and heavy particle temperature versus radial position in the arc for different arc currents; electron temperature measurements (Timmermans et al. [9]) : ■ $I = 40$ A, + $I = 80$ A, $\diamond I = 140$ A, and $\Delta I = 200$ A. Calculations (CARC): --- electron temperature, - - heavy particle temperature.

Mass balance

In the following we consider the balances for electrons (or ions, as we assume a singly ionized ions density and zero negative ion density) and heavy particles, i.e. the sum of ion and neutral density. Thus we take a two fluid approximation. The mass balance then reduces to

$$\nabla \cdot n_h \underline{w}_h = 0$$

and

$$\nabla \cdot n_e \underline{w}_e = \nabla \cdot n_i \underline{w}_i = S_e ,$$

in the electrostatic approximation: $\nabla \cdot \underline{j} = 0$.

If we introduce the mass fluid velocity $\underline{u} \equiv \frac{\sum n_j m_j \underline{w}_j}{\sum m_j n_j}$ then these equations reduce to:

$$\nabla \cdot n_h \underline{u} = 0$$

and

$$\nabla \cdot n_e \underline{w}_e = \nabla \cdot n_i \underline{w}_i = -\nabla \cdot D_a \nabla n_e + \nabla \cdot n_e \underline{u} = S_e ,$$

where D_a is the ambipolar diffusion coefficient. The momentum balance for the heavy particles reduces to the Navier Stokes equation

$$n_h m \underline{u} \cdot \nabla \cdot \underline{u} = -\nabla p + \underline{j} \times \underline{B} - \nabla : \underline{\Pi} .$$

We assume a zero magnetic field and rotation free flow. In the arc a simple

law of Ohm has been assumed $\mathbf{j} = \sigma \mathbf{E}$, but a more complicated situation is being investigated. This is in particular important for the flowing arc, as then a slight divergence of the electric field is to be expected.

The energy equations for heavy particles are

$$\nabla \cdot \frac{5}{2} n_h k T_h \underline{u} + \nabla \cdot \frac{1}{2} m_h n_h u^2 \underline{u} - \nabla \cdot \lambda_h \nabla k T_h + \underline{\Pi} : \nabla \underline{w} = Q_{eh}$$

and for electrons

$$\nabla \cdot \frac{5}{2} n_e k T_e \underline{u} - \underline{u} \cdot \nabla n_e k T_e - \nabla \cdot \lambda_e \nabla T_e = Q_{ohm} + Q_{ion} - Q_{eh} + Q_{rad}$$

In these equations λ_h , λ_e are the thermal heat conductivities, $\underline{\Pi}$ is the heavy particle viscosity tensor, Q_{eh} the electron heavy particle heat transfer, Q_{ohm} the energy source due to Ohmic heating, Q_{ion} the energy sink associated with ionization and recombination, and Q_{rad} the volumetric radiative energy exchange rate.

The model has been tested on a stationary stagnant arc. For such an arc very accurate radially resolved measurements are available [9]. Such a plasma can be observed end on, and by taking two arc lengths, precisions of 2-3% in the temperature and 5-10% in electron density can be obtained. The model results, together with measured data, are shown in Figs. 3 and 4. It is observed that the agreement is satisfactory.

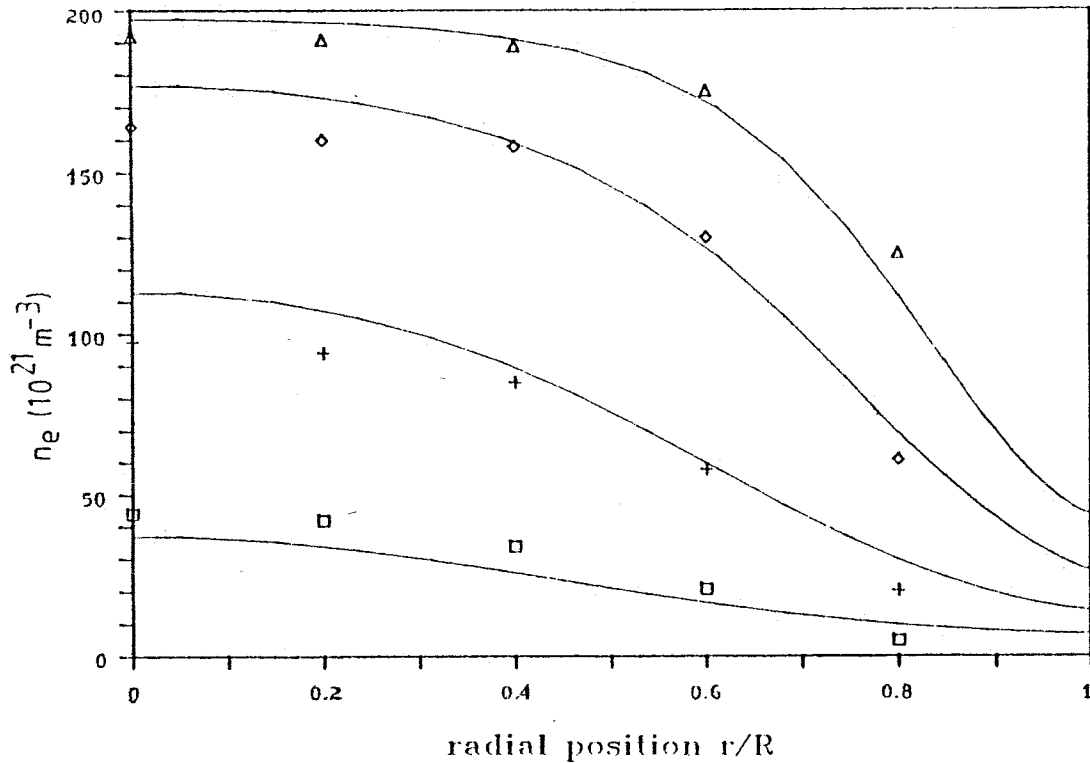


Fig. 4. Stagnation arc: electron density versus radial position in the arc for different arc currents; experiments (Timmermans et al. [9]): ■ $I = 40 \text{ A}$, + $I = 80 \text{ A}$, ◇ $I = 140 \text{ A}$, and △ $I = 200 \text{ A}$. Calculations (CARC) solid lines.

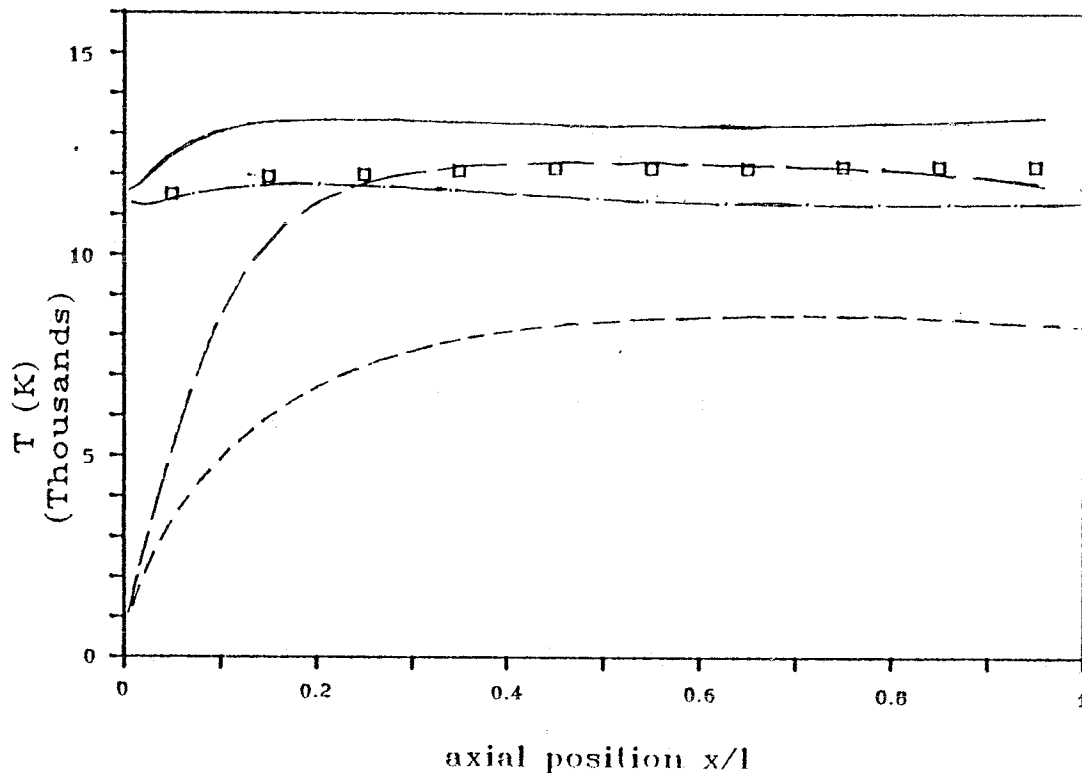


Fig. 5. Flowing arc: variation of the temperature along the arc for an argon flow rate of 100 scc/s. Electron temperature measurements (Kroesen): ■ ; Calculations (CARC): --- center-line electron temperature, - - cross-section average electron temperature, -- -- center-line heavy particle temperature, - - - cross-section average heavy particle temperature.

Of flowing arc only radially averaged values have been measured, as only side on observation through a glass fibre, without the possibility of Abel inversion, was possible. Therefore, we show in Figs. 5 and 6 both the evolution of axial values and the cross section averaged values of plasma parameters. It is expected that at least for low currents the observed values would relate more to the axial values. The measurements (H_{β} broadening for n_e , and line continuum ratio for T_e) sample more the central volume, as there the emissivities are the largest.

Again good agreement is observed except for the higher currents where the model calculations suggest higher (and more peaked) values for the temperature and density than observed. This can be due to an underestimate for the radiation losses and to violation of the assumption $\mathbf{j} = \sigma \mathbf{E}$ which implies $\nabla \cdot \sigma \mathbf{E} = 0$.

EXPANSION

At the anode end of the arc sonic conditions are reached. The plasma expands supersonically and subsequently a shock is formed. After passage of the shock the plasma flows to the substrate with a slowly decreasing velocity. This velocity is still so large that the transit time to the substrate is smaller than 1 ms. At 1 mbar pressure the diffusion of ions in a neutral

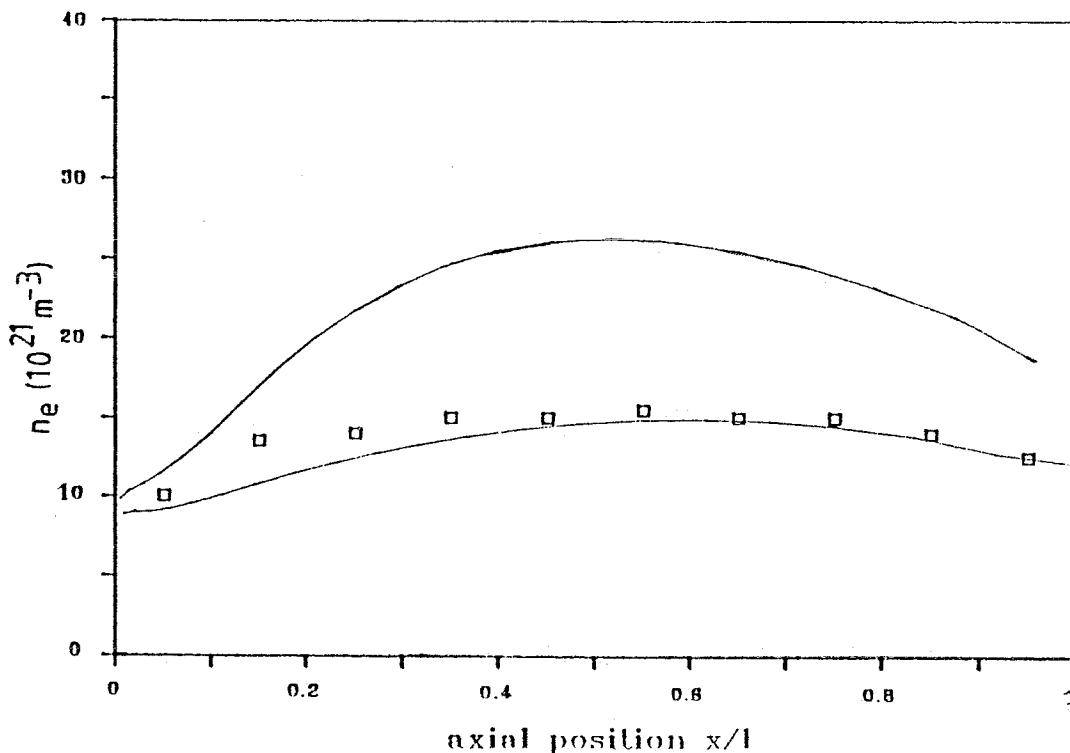


Fig. 6. Flowing arc: variation of the electron density along the arc for an argon flow rate of 100 scc/s. Experiments (Kroesen): ■ ; Calculations (CARC): --- center-line electron temperature, --- cross-section average electron density.

background is governed by ion-neutral (charge exchange) collisions, which leads to parabolic increase of the plasma diameter (cf. Fig. 1). Typical cross section areas of 100 cm^2 are reached at the substrate position. In atomic gases, such as argon, the radiative and dielectronic recombination is slow, and can be ignored in the first instance. For partially molecular gases the situation is different. By non resonant charge transfer molecular ions will be formed which dissociatively recombine with electrons. This process is highly effective for electron densities above $10^{16}/\text{m}^3$, so the electron density decreases fast to that value and stabilizes then.

If in a deposition process ions (and electrons) are to be important then the best approach would be to have atomic ions only. Injection of monomers in the arc, full dissociation, and considerable ionization are then required.

If only radical formation and radical fluxes are needed, then downstream injection is a possibility. Then, molecular fragments can survive and it is possible to retain some of the chemical structure of the monomer.

EXAMPLES OF DEPOSITION PROCESSES

In conclusion we will give several examples of plasma deposition.

First amorphous carbon has been deposited [3,4] with large rates: up to 40 nm/s for methane as monomer, and up to 200 nm/s for C_2H_2 as

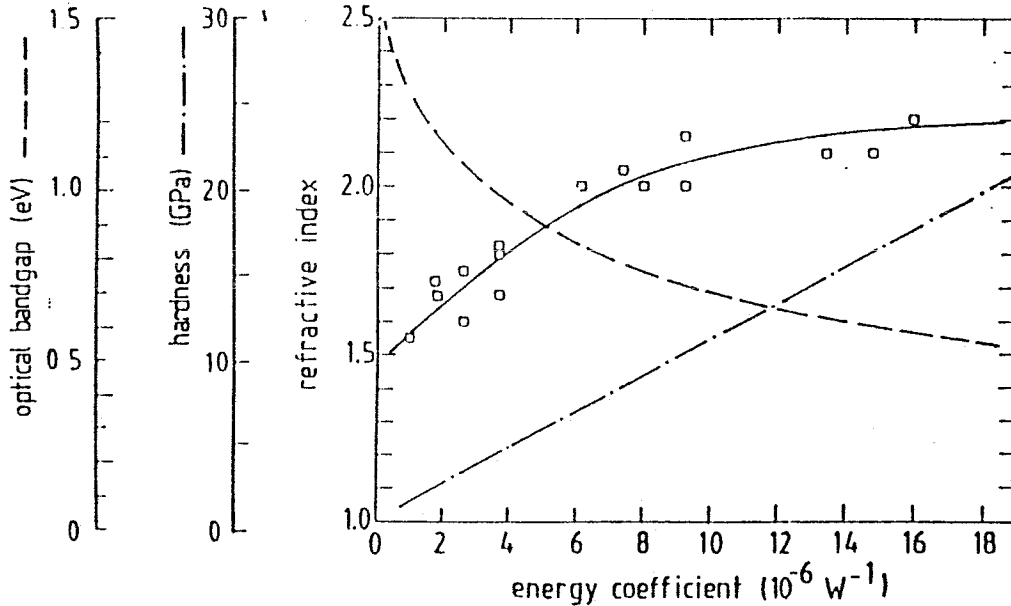


Fig. 7. Optical bandgap, hardness and refractive index as a function of the inverse energy coefficient.

monomer. The resulting qualities can be summarized as given in Fig. 7, in which hardness, index of refraction and bandgap are shown as functions of the inverse energy ratio Q . This quantity is defined as the ratio of the carbon flow and the product of argon flow and power input.

$$Q \equiv \frac{[\text{carbon flow}]}{p[\text{argon flow}] \times \text{power}} \left[\frac{1}{\text{W}} \right]$$

Since this product is a measure of the energy flow in the first section of the arc, the ratio Q is a measure of the inverse of the energy in the flow per carbon particle (ion). Note also that a minimum is required for this quantity: the energy flow must be large enough to dissociate and ionize the monomer completely: 75 eV/C for CH_4 and 35 eV/C for C_2H_2 . The difference between these values explains also the difference in maximally obtainable growth rate for those two monomers (Fig. 8). So, even though the deposition method is vastly different, the material qualities are very similar to those of classically obtained materials.

Amorphous carbon (diamond-like) results if the substrate is in the room temperature range (below 100°C). If the substrate is heated to 1000°C , and H_2 gas is fed into the arc, diamonds are formed [5], either single crystals or polycrystalline material. Growth rates are typically 10 nm/s at surfaces of 1 cm^2 .

At intermediate temperatures graphite is deposited. In this case the hydrogen admixture has to be small. In some circumstances deposition rates of 500 nm/s over a surface of 4 cm^2 have been obtained.

Recently amorphous hydrogenated silicon has been deposited with the same method. In view of pyrophonic and toxic properties of SiH_4 a mixture of 5% SiH_4 in argon gas has been used. It is injected through a ring which is mounted 5 cm downstream the nozzle.

With the relatively small monomer flow of .15 scc/s SiH_4 in 3 scc/s argon and a main carrier gas flow of 100 scc/s, argon deposition rates of 10 nm/s

have been achieved. The properties of the layers are being investigated with ellipsometry in the infrared and UV visible range, a.o. as a function of the substrate temperature. Bondings of SiH_2 and the to be preferred SiH are being observed. Further investigations are in progress.

As a conclusion it appears that separate plasma production and deposition leads to a fast deposition process, with which several types of thin layers can be made.

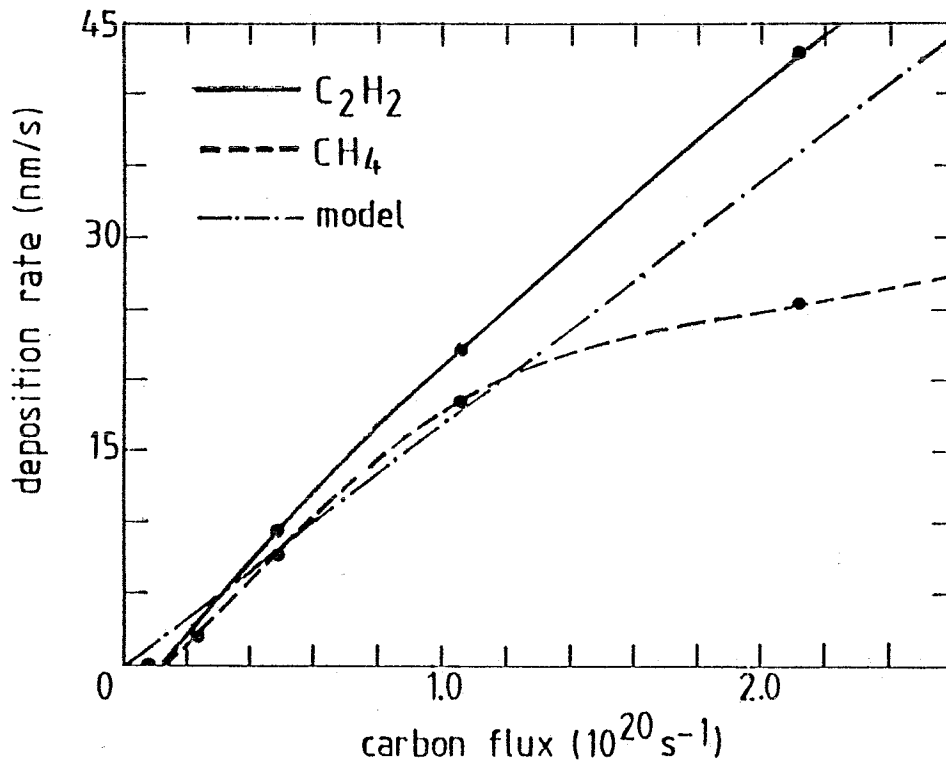


Fig. 8. Deposition rate as a function of the injected carbon flux.

REFERENCES

- [1] Zalm, P.C. *Pure & Appl. Chem.* **57** (1985) 1253.
- [2] Cf. Invited Papers of ISPC conferences: ISPC-7 Eindhoven (1985), published in *Pure & Appl. Chem.* **57** (1985); ISPC-8 Tokyo (1987), published in *Pure & Appl. Chem.* **60** (1988).
Schram, D.C., Hoog, F.J. de, Bisschops, T.H.J., Kroesen, G.M.W., *Proc. SASP, Obertraun* (1986) 181.
Schram, D.C., Bisschops, T.H.J., Kroesen, G.M.W., Hoog, F.J. de, *Plasma Physics & Contr. Fusion* **29** (1987) 1353.
- [3] Kroesen, G.M.W.. *Plasma Deposition: Investigations on a New Approach*, Thesis Eindhoven University of Technology, The Netherlands (1988).
- [4] Kroesen, G.M.W., Schram, D.C. and Sande, M.J.F. van de. *Fast Deposition of Amorphous Hydrogenated Carbon Films Using a Supersonically Expanding Arc Plasma*. *Plasma Chem. & Plasma Proc.* **10** (1990) 49-69.

- [5] Bachmann, P.K., Beulens, J.J., Kroesen, G.M.W., Lydtin, H., Schram, D.C. and Wiechert, D.U. Diamond Deposition from a Cascaded Arc DC Plasma. Proc. 3rd Conf. on Surface Modification Technologies, Neuchatel, Switzerland (1989).
- [6] Meeusen, G.J., Wilbers, A.T.M., Timmermans, C.J. and Schram, D.C., to be published.
- [7] Fauchais, P., Private communication.
- [8] Milojevic, D., Schram, D.C. and Vallinga, P.M. A two-dimensional non-equilibrium model of cascade arc plasma flows, to be published.
- [9] Timmermans, C.J., Rosado, R.J. and Schram, D.C. An investigation of non-equilibrium effects in thermal argon plasmas. *Z. Naturforschung* **40A** (1985) 810-825.